Covalence in the $[Cr(CN)_6]^{3-}$ Ion studied by *X*-Ray Diffraction from $Cs_2KCr(CN)_6$†

Brian N. Figgis* and Philip A. Reynolds
School of Chemistry, University of Western Australia, Nedlands, W.A. 6009

A high-precision *X*-ray diffraction data set on the compound $Cs_2KCr(CN)_6$ has been collected at 120 K, and analysed in terms of the charge-density distribution and chemical bonding features. It has been useful to model the density only at the level of cubic symmetry, *viz.* a regular octahedral $[Cr(CN)_6]^{3-}$ ion, because small effects, apparently arising from anharmonic motion, perturb the data with high values of *h*, restricting the resolution along the *a* axis for charge-density purposes. Molecular form-factors have been derived for the CN^- ion by fitting the theoretical electron density by a multipole analysis, enabling a more critical comparison between experiment and theory than is usual. In the region of the chromium atom and its six bonded carbon neighbours the density may be described by the superposition of a 'prepared' $t_{2g}^3e_g^0$ Cr^{3+} ion and the unco-ordinated cyanide ions, with some σ donation and π back donation resulting in $t_{2g}^{2.3(4)}e_g^{0.6(5)}$. On the nitrogen atoms of the cyanide ions significant charge [0.3(1) e] appears to have been polarised from the π orbitals into the σ 'lone pair,' probably by the 'intramolecular' influences of the cations of the crystal. These cations are themselves perturbed away from simple spherical 1+ charged species by the contacts with the nitrogen atoms.

The study of covalence in metal–ligand bonding in transition-metal complexes has been considerably advanced over the years by the interaction of theoretical treatments with spectroscopic results. More recently, diffraction methods have commenced to give direct and unique information on the charge (*X*-ray diffraction) and the spin (polarised neutron diffraction) density distributions in such complexes. The comparison of these simple, fundamental, properties with theoretical wavefunctions provides a very different test of these and also a new perspective. The information contained in the ground-state spin and charge densities provides a stringent test of theory.

The hexacyanochromate(III) ion provides an excellent experimental system for study by diffraction methods. The M–CN bond is thought to be highly covalent in relationship to such systems, it includes both σ and π components, the complex ion is small and highly symmetrical, it has a moderately high spin ($S = \frac{3}{2}$), and large crystals containing it may be grown.

In previous papers we have analysed the charge density in $[Co(NH_3)_6][Cr(CN)_6]$ and $[Co(NH_3)_5(OH_2)][Cr(CN)_6]$[1] and the spin density in $Cs_2KCr(CN)_6$.[2,3] These results have been compared to recent theoretical calculations, both restricted Hartree Fock (RHF)[4,5] and DV-Xα.[6]

The spin-density experiment showed a complex pattern in which there is *negative* spin in the CN unit σ framework, net positive spin in its π framework, while the chromium $3d$-$t_{2g}(\pi)$ population is reduced from the free-ion value of 3.0 and expanded 8% radially, and there is a substantial diffuse component. These observations are compatible with π backbonding from Cr t_{2g} orbitals into the ligand π orbitals, while the Cr e_g σ bond to the ligand is spin-polarised by about the same amount. The observed negative spin is incompatible with the RHF calculations, but overall the experimental spin density agrees quite well with the DV-Xα results.

The charge-density[1] experiment reveals strong σ-bonding and weaker π-bonding effects concerning the chromium atom, and agrees satisfactorily with both types of calculation in that regard. It also reveals strong polarisation of the electron density in the cyanide units from the σ to the π system. Neither calculation accounts for this. In addition, both calculations underestimate by a factor of about two the observed covalent spin and charge transfers from the chromium atom.

The errors in the charge-density experiment preclude the precise assessment of these covalence parameters which is available in the spin-density case. In addition, in other systems ($FeCl_4^-$,[7] $CoCl_4^{2-}$[8]) the charge density appears noticeably to be affected by the neighbouring ions, an 'intermolecular' effect. In order to provide a futher independent estimate of the covalent charge transfers (in addition to the two complexes in ref. 1), and to investigate the intermolecular effects more deeply, we have measured the charge density in $Cs_2KCr(CN)_6$ and present the results in this paper.

In an attempt to improve the methods of comparison of theory with experiment, in this paper we have used *molecular* form-factors for the unco-ordinated cyanide ion in making our estimate of charge migrations in the bonding of the six cyanide ions to the chromium(III) ion. This procedure reduces the uncertainty associated with the substantial deformation density of the C≡N bond in the 'free' cyanide ion.

Experimental

Amber rectangular-prismatic crystals of $Cs_2KCr(CN)_6$ were grown by slow cooling of a solution of $K_3Cr(CN)_6$ containing 2 mol of CsCl per mol of that compound. A specimen of approximately cube shape, with the dimensions given in Table 1, was mounted on a Syntex $P2_1$ four-circle *X*-ray diffractometer equipped with a locally developed nitrogen-gas cooling attachment. The cell constants were determined by a least-squares refinement of the setting angles of six high-angle reflections. A complete sphere of data, with some small segments missing, was collected to a $(\sin\theta)/\lambda$ maximum of 10.8 nm^{-1}. The specification of standards, scan widths, and other parameters was as described previously.[9] The lack of variation in standards indicated negligible crystal decomposition during the course of the experiment. Crystal and other experimental data are given in Table 1. The data were processed using the

† Dicaesium potassium hexacyanochromate(III).

Supplementary data available: see Instructions for Authors, *J. Chem. Soc., Dalton Trans.*, 1987, Issue 1, pp. xvii—xx.

Table 1. Crystal and experimental data for $Cs_2KCr(CN)_6$

T/K	120(5)
Stability in T/K	2
Crystal dimensions/mm	
(100) to ($\bar{1}$00)	0.23
(011) to (0$\bar{1}\bar{1}$)	0.25
(0$\bar{1}$1) to (01$\bar{1}$)	0.25
Unit cell	
a/nm	1.1199(4)
b/nm	0.8301(3)
c/nm	0.7703(2)
β/°	90.82(2)
U/nm^3	0.7160(5)
Space group	$P2_1/n$, $Z = 2$
λ(Mo-$K_{\bar{a}}$)/pm	70.069
M	513
D_m/g l^{-1}	2.33(1)
D_c/g l^{-1}	2.34
F(000)	462
No. reflections measured	17 587
No. unique reflections	6 586
$[\sin\theta/\lambda]_{max.}$/nm^{-1}	10.4
μ(Mo-$K_{\bar{a}}$)/mm^{-1}	6.08
Transmission factor	0.23—0.36

Table 2. Fractional atomic co-ordinates ($\times 10^4$)

Atom	x	y	z
Cr	0	0	0
K	0	5 000	5 000
Cs	2 525(1)	4 223(1)	−261(1)
C(1)	368(3)	1 319(3)	−2 197(3)
C(2)	469(3)	−2 095(3)	−1 287(3)
C(3)	1 743(3)	282(3)	842(3)
N(1)	593(5)	2 048(5)	−3 444(5)
N(2)	761(4)	−3 251(4)	−2 019(5)
N(3)	2 711(3)	481(5)	1 312(5)

XTAL system of computer programs,[10] to give a final equivalent-averaged set.

Since this is a highly absorbing crystal, the absorption correction was refined. Under the microscope the crystal faces appeared mirror-flat. The measured crystal dimensions were successively changed so that the agreement between monoclinic equivalents, $R_I = \Sigma$av.$|I - $ av.$(I)|/\Sigma$av.(I) (av. = average) was minimised for 100 selected reflections. Although the changes in crystal dimensions from the optically determined values were within the errors of that measurement, a significant improvement in R_I was obtained. The symmetry averaging gave $R_I = 0.022$ and $\Sigma\sigma(I)/\Sigma I = 0.017$ for the final complete data set of 6 586 unique reflections.

Structure Refinement.—In order to examine valence effects we require a knowledge of the core-electron position and thermal parameters. Since the high-angle data are relatively unaffected by valence effects, we used the 4 058 data with $(\sin\theta/\lambda) > 7.5$ nm^{-1} to estimate these parameters. A refinement of positional and thermal parameters minimising $\Sigma\sigma(I_{obs.})^{-2}(I_{obs.} - I_{calc.})^2$ was performed using the program ASRED. Ionic scattering factors,[11] modified for anomalous dispersion,[12] were employed. For carbon and nitrogen, neutral atoms augmented by one half of a 2s electron were used, better to represent CN^-. As a rough correction for multiple scattering a refineable constant intensity was subtracted from all the data. An isotropic extinction correction was also refined. We obtained $R'(I) = 0.095$, $R(F)[I > 3\sigma(I)] = 0.053$, and $\chi = 1.29$. The final atomic co-ordinates are listed in Table 2.

Table 3. Interatomic distances (pm) and angles (°). The figures in square brackets refer to the ambient-temperature structure[13]

(*i*) Bonding contacts

Cr–C(1)	206.2(4) [207.5(4)]	C(1)–N(1)	116.6(5) [113.8(6)]
Cr–C(2)	207.4(5) [207.2(4)]	C(2)–N(2)	116.3(5) [113.8(6)]
Cr–C(3)	206.2(5) [206.8(4)]	C(3)–N(3)	115.0(5) [113.7(6)]

(*ii*) Angles

C(1)–Cr–C(2)	89.9(2) [90.1(2)]	Cr–C(1)–N(1)	178.8(6) [178.5(6)]
C(1)–Cr–C(3)	90.1(2) [90.1(2)]	Cr–C(2)–N(2)	178.2(7) [179.5(8)]
C(2)–Cr–C(3)	90.0(2) [89.7(2)]	Cr–C(3)–N(3)	178.3(4) [177.6(4)]

(*iii*) Non-bonded contacts

Cs • • • N(2^{I})	317.3(4) [320.8(4)]	K • • • N(2^{IV})	283.8(4) [285.5(4)]
Cs • • • N(3)	334.2(4) [337.9(5)]	K • • • N(1^{V})	280.5(4) [281.7(4)]
Cs • • • N(3^{II})	323.0(4) [325.6(4)]	K • • • N(3^{II})	279.8(4) [281.2(4)]
Cs • • • N(1^{III})	331.7(4) [334.0(4)]		

Transformations of the asymmetric unit: I x, 1 + y, z; II 0.5 − x, 0.5 + y, 0.5 − z; III 0.5 − x, 0.5 + y, −0.5 − z; IV x, 1 + y, 1 + z; V x, y, 1 + z.

Extinction was negligible, and the multiple scattering was very small, but positive as expected. Table 3 shows the bonding contacts and angles, and the shortest non-bonded contacts. The second entry in each case, in square brackets, is the ambient-temperature result.[13]

Results

The Structure.—The structure of this and other Elpasolites has been discussed at length elsewhere.[13–16] For the purposes of the valence-electron analysis we need to note two general points.

First, the $[Cr(CN)_6]^{3-}$ ion is close to octahedral in stereochemistry, even though in the space group $P2_1/n$ the site symmetry is only inversion. There are, however, small but significant bond-length differences. The non-bonded environment of the $Cr(CN)_6$ unit is also close to cubic in symmetry. Each nitrogen atom has an approximately linear C–N • • • K contact, shown in Table 3. In addition, each nitrogen atom has three close and one longer Cs • • • N contact nearly at right angles to the C–N axis. As a very rough approximation we can describe each cyanide unit as having a distorted octahedral environment, with Cr(1) and K(1) axial and three or four Cs(1) equatorial neighbours, derived by small distortions from the high-temperature cubic $Fm3m$ phase.

Secondly, at ambient temperature we noted[13] substantial anharmonic effects which could be rationalised in terms of the known phase transitions in Elpasolites.[14] A large (1 300 e nm^{-3}) peak in the deformation density at $(\frac{1}{4}, \frac{1}{2}, 0)$ shows that at ambient temperature the caesium ion is not moving harmonically, but that there is some anharmonicity or disorder along b, probably as a precursor to the $P2_1/n \longrightarrow P4mnc$ transition at higher temperatures where Cs^+ occupies $(\frac{1}{4}, \frac{1}{2}, 0)$. In addition, both chromium and potassium showed anharmonic effects.

In Figure 1 we show, for the 120-K data, the charge density in the $z = 0$ plane which contains Cr(1) and K(1) and almost contains Cs(1). The latter still shows evidence of the anharmonicity, although the peak height, 800 e nm^{-3}, is reduced from the ambient-temperature value. Around K(1), the excess density reduces from 1 100 to 300 e nm^{-3} while at Cr(1) the pattern changes from a hole of −500 to a peak of 400 e nm^{-3} along a. It is clear that, especially for the caesium and chromium ions, in the charge-density experiment the reduction in temperature to 120 K has not reduced the 'anharmonic' effects to negligible proportions. For each of the three atoms the anharmonicity

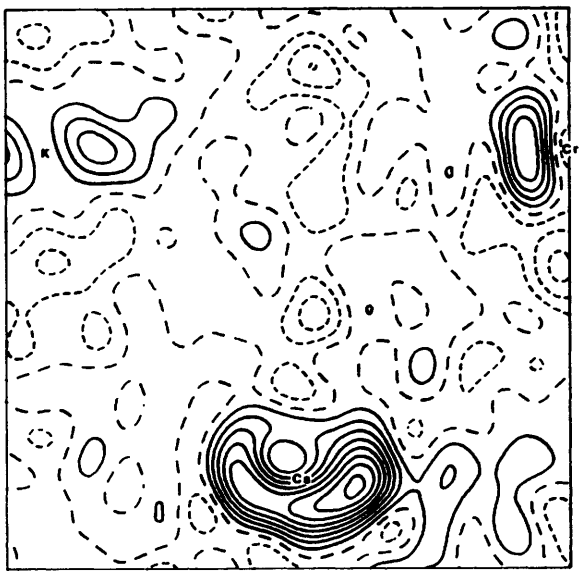

Figure 1. The experimental charge-deformation density in the $z = 0$ plane. Contour interval 100 e nm^{-3}; solid lines for positive, dashed for zero, and dotted for negative density. The dimensions of the map are 600 × 600 pm, covering $-0.54 < x < 0$ (horizontal), $-0.54 < y < 0.18$. The Cs atom shown is just out of the plane

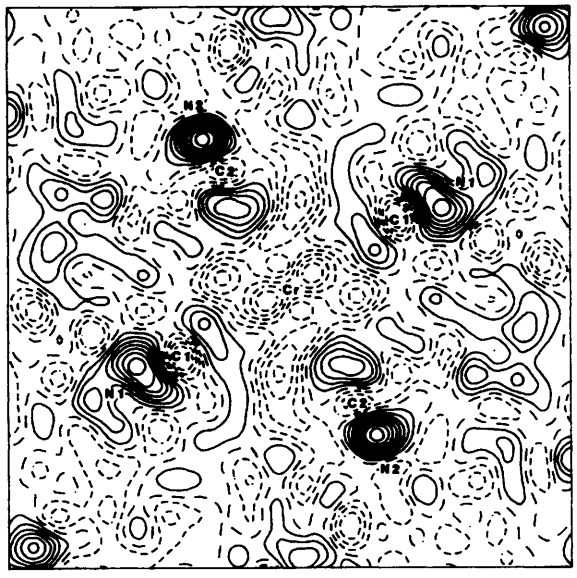

Figure 2. The deformation density in the Cr(1), C(1), N(1), C(2), N(2) least-squares plane. The map is of dimensions 880 × 880 pm, centred on Cr(1). Contour details as for Figure 1

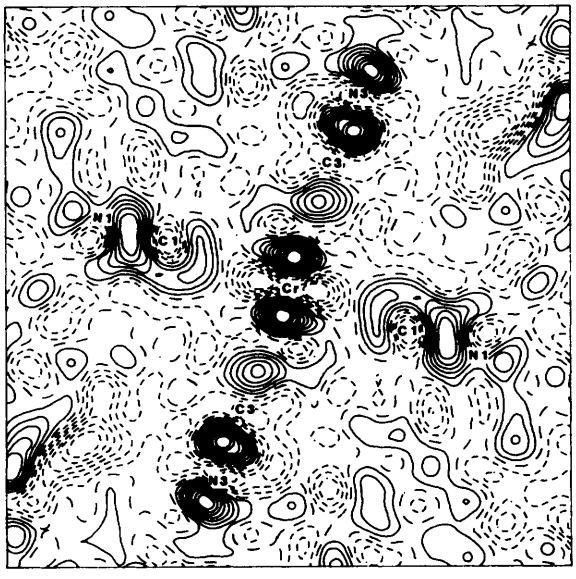

Figure 3. The deformation density in the Cr(1), C(1), N(1), C(3), N(3) plane, as for Figure 2

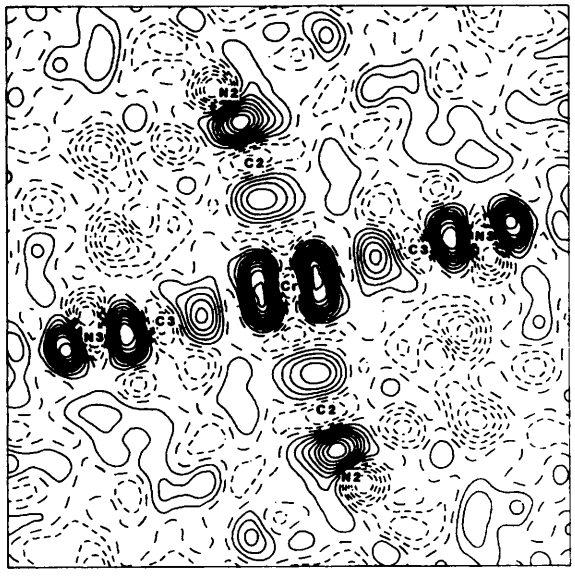

Figure 4. The deformation density in the Cr(1), C(2), N(2), C(3), N(3) plane, as for Figure 2

now appears to be dominant along *a*. The reduction in temperature seems to have removed much of the anharmonic behaviour along *b* for Cs(1), leaving a residue along *a*. We have investigated the 'anharmonicity' further by attempting to model it as multiply twinned *P*1 crystals, after the manner that was successful for $K_3Cr(CN)_6$,[17] but without success. A simple model involving terms in h,[4] reflecting anharmonic motion along *a*, produces a distinct improvement in fit. This supports anharmonicity as the origin of the excess densities observed, but a more rigorous treatment of anharmonicity was not attempted. We conclude that there is some anharmonicity or disorder affecting the reflections with higher values of h and hence concerned with displacements along *a*. The effect on the $Cr(CN)_6$ fragment deformation charge density is illustrated in Figures 2—4. In Figure 2, which shows the Cr(1), C(1), C(2) plane, there is approximate four-fold symmetry. This plane is approximately perpendicular to *a*, since Cr(1)–C(3) lies nearly along *a*. The related planes Cr(1), C(1), C(3) (Figure 3) and Cr(1), C(2), C(3) (Figure 4) show a distinct lack of four-fold symmetry and the concentration of density along the *a* axis suggested by Figure 1.

The implication of the preceding paragraph for the charge-density modelling is that all high-h data must be discarded, being affected by the anharmonicity. Accordingly, we use only

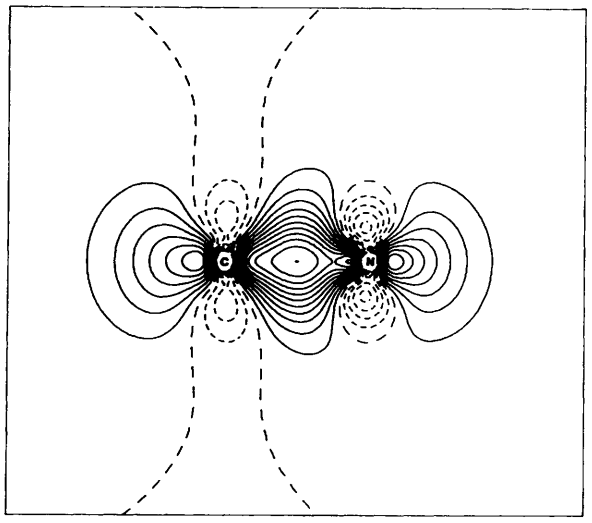

Figure 5. The theoretical deformation density for the cyanide ion. Contour details as in Figure 1

the 780 data with $h < 4$ and $(\sin\theta)/\lambda < 7.5$ nm^{-1} in our valence-orbital modelling. The resulting loss of resolution along a means that we will not employ models of the $Cr(CN)_6$ charge density of symmetry lower than cubic.

Cyanide Ion Form-factor.—The theoretical deformation density derived from a near-HF limit calculation for the CN^- ion is shown in Figure 5.[15] It reaches peak heights of 1 100 e nm^{-3}. If we wish to observe the changes in bonding of a Cr^{3+} ion with CN^- ions, clearly it would be advantageous to use as a promolecule, rather than spherical Cr, C, and N atoms, a prepared $t_{2g}^3e_g^0$ chromium unit and 'molecular' unco-ordinated cyanide ions. This procedure requires the calculation of molecular form-factors for the unco-ordinated cyanide ions in the crystal lattice. We have fitted the density of Figure 5 by least-squares methods with a series of atom-centred radial-density functions and multipoles. The resulting multipolar radial functions can be Fourier transformed to give a set of atomic, multipolar, form-factors,[9] $\langle j_m \rangle$. The set of $\langle j_m \rangle$ can then be used to calculate the scattering from the unco-ordinated cyanide ions in the crystal, with appropriate thermal motions applied, using the parameters from the high-angle refinement.

A grid of 1 481 density values for the calculated cyanide ion[18] was used. In all the calculations, cylindrical symmetry of the cyanide ion was imposed. A fit using the atomic carbon and nitrogen 2p wavefunctions of Clementi and Roetti[19] (*i.e.* j_0 and j_2 on each atom, with one radial function) gave a poor result ($R = \Sigma|\rho_{calc.} - \rho_{fit}|/\Sigma\rho_{calc.} = 0.0460$). The model deformation density, while qualitatively similar to the complete theoretical density, gave peaks or troughs of only half its size. Given the relative failure of minimal basis sets in Hartree-Fock calculations, that result is not unexpected.[20] We therefore expanded our description to seven radial functions on each atom, three multipoles (j_0, j_1, and j_2) on all radial functions, and two further angular functions (j_3 and j_4) on the very diffuse functions, 50 parameters in all. The radial functions used were 2p [$R_{2p}(r)$], 1s [$R_{1s}(r)$], two contracted 2p functions [$R_{2p}(r/2)$, $R_{2p}(r/4)$], and two Gaussians of mean-square width 2 000 and 4 000 pm^2. These functions were selected from a complete set of $R_{1s}(r)$, $R_{2p}(r/2^n)$, and Gaussians of width 8 000/n pm^2 with n = 1—4, such that they were not highly correlated with each other and gave significant coefficients in preliminary fits. The fit to the experimental charge density was much improved, R = 0.006, but the individual coefficients have no direct physical meaning.

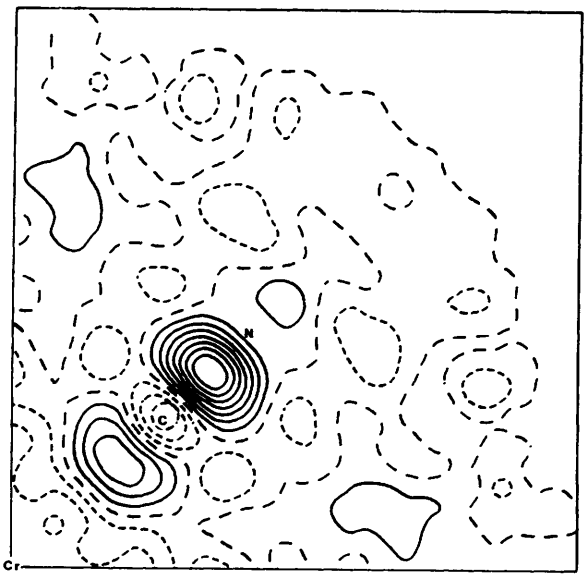

Figure 6. The averaged deformation density in the Cr(1), C(1), C(2) plane. Contour details as in Figure 1

The fit has about the same errors as the uncertainties in the theoretical calculation arising from the neglect of correlation,[21] so it is satisfactory for our purposes. After analytical Fourier transformation, we summed the individual radial components to give a set of ten molecular multipolar form-factors. These form-factors were used in the program ASRED in exactly the same way as normal anisotropic valence-orbital scattering functions. The multipolar description gives charges on C and N of −0.494 and −0.506, compared to the theoretical populations, obtained using a Mulliken population analysis, of −0.502 and −0.499. Although the agreement is good both procedures are arbitrary decompositions of the molecular charge density and are not comparable on any rigorous basis.

Valence-electron Refinement.—In Figure 2, which shows the $Cr(CN)_4$ plane least affected by anharmonicity, we see the appropriate four-fold symmetry of the deformation density. In order to clarify the bonding detail, assuming cubic symmetry for the $Cr(CN)_6^{3+}$ ion, we have averaged this deformation density over all the Cr–C–N units. The resulting density is shown in Figure 6. The averaging process reduces the errors in the maps but may conceal real non-cubic effects. The thermal smearing of the static deformation density increases from Cr through to N. When Figures 5 and 6 are compared we see a great similarity in the cyanide-unit region. There are three peaks in the σ-bonding region, with the mid-bond peak highest in each case, together with a depopulation of the π orbitals relative to σ. In the presence of these strong unco-ordinated cyanide features there are no obvious qualitative effects from the bonding to the chromium(III) ion. We have therefore undertaken valence-orbital refinements of the data using the program ASRED. As a benchmark, the agreement factors were calculated for the spherical atom model based upon the ions Cr^{3+}, $C^{0.5-}$, $N^{0.5-}$, K^+, and Cs^+, with 780 data, refining only the scale factor and a caesium population on the K(1) site, which we shall call refinement R1. The caesium contamination of the K(1) site amounted to 6%. We obtained R = 0.047, R' = 0.065, and χ = 3.68.

We then used the cyanide molecular form-factors described above, and refining the same two variables yielded R = 0.040, R' = 0.053, and χ = 2.99. This refinement, R2, is a significant improvement, as expected from an examination of Figure 6.

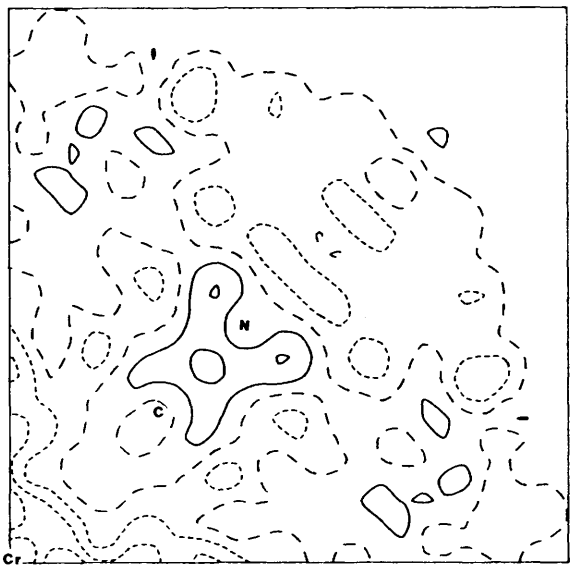

Figure 7. The averaged residual charge density in the Cr(1), C(1), C(2) plane. Contour details as in Figure 1

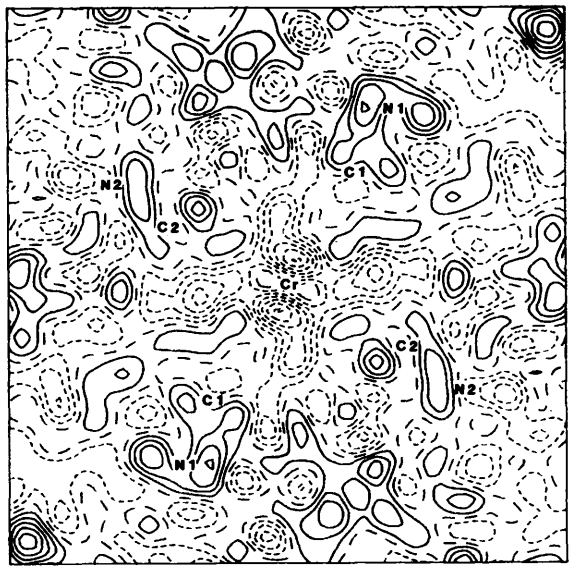

Figure 8. The residual density in the Cr(1), C(1), C(2) plane. Contour details as in Figure 1

Table 4. Results of the valence-orbital refinement (R3), normalised to populations in electrons

Cr	$3d\text{-}t_{2g}$	2.3(4)	N(1)	$(sp)_1$	0.2(1)
	$3d\text{-}e_g$	0.6(5)		$(sp)_1$	0.0(1)
	P_{shell}	0.1(4)		$2p_\pi$	−0.4(1)
	K_{3d}	0.94(1)		P_{shell}	0.2(2)
				K_{sp}	0.97(3)
C(1)	$(sp)_1$	−0.2(1)			
	$(sp)_2$	0.0(1)	Cs	'6s'	0.0(4)
	$2p_\pi$	−0.1(1)		P_{shell}	0.5(1)
	P_{shell}	0.3(1)			
	K_{sp}	0.96(2)	K	'6s'	0.066(3)
				P_{shell}	0.3(1)
			Cr–C	'Overlap'	0.2(1)

To estimate the effect of the Cr–CN bonding we then introduced valence-orbital parameters. On the carbon and nitrogen atoms were placed $(sp)_1$, $(sp)_2$, and $2p_\pi$ orbitals, where $(sp)_1$ is an *sp* hybrid orbital directed at the chromium atom, $(sp)_2$ a hybrid directed away from the chromium atom, and $2p_\pi$ are the pair of *p* orbitals describing cylindrical density in the plane perpendicular to $(sp)_{1,2}$. On the chromium atom we refined $3d\text{-}t_{2g}$ and $3d\text{-}e_g$ populations, and on the caesium atom a '6*s*' population. All form-factors were derived from the wavefunctions of Clementi and Roetti. In addition we refined radial parameters for the chromium *d* orbitals and the carbon and nitrogen *s*/*p* orbitals. These latter parameters, K_{nl}, expand ($K > 1$) or contract the density on the centre uniformly. In the Cr–C mid-bond region we placed a refinable population with H-1*s* radial dependence to model overlap density. The *X*-ray diffraction study on Cs_2CoCl_4[8] revealed substantial intermolecular polarisation effects, particularly of the caesium ions, the spherical component of which could be partially represented by a population in a thin shell of electron density at 150 pm from each atom, P_{shell}. Such shells were introduced into the present model. We have not included 4*s* or 4*p* functions although these have been shown to be important in other systems, where the oxidation state of the metal is formally +2.[8] Both theoretical studies[4] and our previous charge-density study of the $[Cr(CN)_6]^{3-}$ ion[1] indicate little 4*s* or 4*p* participation in the bonding. The point is more fully discussed in ref. 1. Attempts at inclusion of such functions in the present refinements are not reported since their correlation with the P_{shell} parameter is significant. The correlation arises because of the restricted nature of the data we have used ($h < 4$) compared with that of ref. 1.

There resulted a 20-parameter refinement, R3, which gave $R = 0.040$, $R' = 0.045$, and $x = 2.60$, the details of which are set out in Table 4. The improvement in fits between refinements R3 and R2 is about half that between refinements R2 and R1. In order to compare with the previous *X*-ray diffraction work on the $[Cr(CN)_6]^{3-}$ ion[1] we performed a similar refinement but without using the molecular cyanide form-factors or the P_{shell} parameters. The resultant refinement, R4, gave $R = 0.038$, $R' = 0.046$, and $\chi = 2.66$.

The averaged residual density from refinement R3 is shown in Figure 7 and the residual density in the Cr(1), C(1), C(2) plane in Figure 8. The residual density of Figure 7 is much reduced from the deformation density in Figure 6: for example the CN mid-bond peak is reduced from 700 to 200 e nm^{-3} and the 'lone pair' peaks have disappeared. The residual density from refinement R2 (not shown) is very similar to that of Figure 7, supporting the previously mentioned observation that most of the features in the $Cr(CN)_6$ region are explicable in terms of Cr^{3+} and uncoordinated CN^- ions; the *maps* show little obvious evidence of Cr–CN bonding. The individual-atom refinement R4 gives peaks intermediate between those of Figures 6 and 7. It seems that the valence-orbital functions cannot quite fit the $Cr(CN)_6$ unit density, but the residuals in this area do not have an appreciable effect on the goodness-of-fit of the model.

Discussion

In Table 4 we see that the electron density has been partitioned by our model to give a charge of +0.5(1) on Cs(1), +0.7(1) on K(1), and −1.7(2) on the $Cr(CN)_6$ unit, indicating that significant charge transfer to the alkali-metal ions has taken place. However, the charge so transferred resides largely in the diffuse 'shell' orbitals and so should be regarded as associated with bonding phenomena rather than as simple ionisation. This is indicative of significant 'intermolecular' effects on the $Cr(CN)_6$

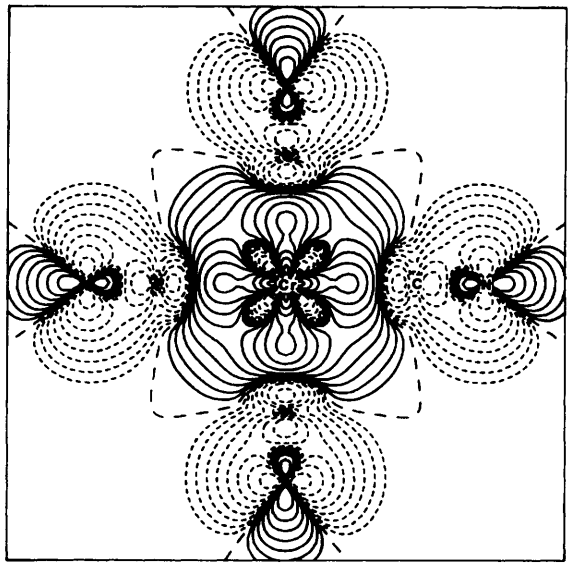

Figure 9. The static modelled charge density in the $Cr(CN)_4$ plane after the subtraction of a 'prepared' $t_{2g}^3e_g^0$ Cr^{3+} ion and six 'theoretical' cyanide ions, *viz.* the 'model residual density.' Contours are logarithmic, the Nth contour being at $2^{(N-13)}$ e a.u.$^{-3}$, *i.e.* the first at 120×10^{-6}, the seventh at 16×10^{-3} e a.u.$^{-3}$ (0.11 e Å^{-3})

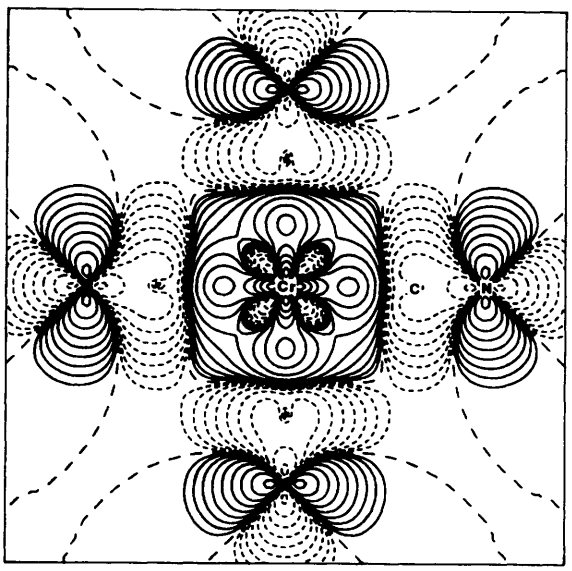

Figure 10. The model residual density in the $[Cr(CN)_6]^{3-}$ ion in the cobalt ammine salts[1]

unit. Table 4 shows that the results are, to a first approximation, consistent with a $Cr(t_{2g}^3e_g^0)$ atom surrounded by six free-ion-like cyanide ions. There are small but significant differences from that description, due to Cr–CN bonding, which are evident in the values of the refined parameters although not in the maps. The differences constitute a significant loss of density from Cr d_π and gain into Cr d_σ orbitals, with small changes in the cyanide ligands. We can rationalise these observations, broadly, in terms of three parameters: a σ donation of 0.17(8) e from each cyanide unit to the chromium atom, $q(L_\sigma \rightarrow M_\sigma)$, a weaker π 'back donation' of 0.09(6) e from chromium to cyanide groups, $q(M_\pi \rightarrow L_\pi)$, and a substantial reorganisation, 0.3(1) e, of the cyanide unit density from π to σ, $-q(L_\sigma \rightarrow L_\pi)$.

The value of σ donation is in fairly good agreement with our earlier experiment[1] and with theory. The π back donation is also in accord with the earlier experiment, but theory appears to underestimate this part of the bonding. The overlap, which theory assigns as mainly σ, is also in agreement with both theory and the earlier experiment.

We can conclude that the Cr–CN bonding is consistently estimated well by experiment, but that theory does not account adequately for the π backbonding. Such differences between diffraction experiments and theory are consistent with a number of other studies reviewed in ref. 22.

In Figure 9 we show a map of the difference between the static experimental model charge density and that of an assemblage of a $t_{2g}^3e_g^0$ chromium ion and six 'free' cyanide ions. A similar, theoretical, diagram is given in ref. 5. The chromium(III) ion density is similar in the two diagrams but there are distinct differences in the cyanide region. In Figure 10 we give a similar map from the results of the experiment relating to salts of cobalt ammine cations.[1] The Cr–C regions are very similar in both but there are obvious differences around the nitrogen atoms. The cobalt ammine salts show a depletion of electrons in the nitrogen σ-bonding 'lone pair' region and enhancement in the π orbitals, but here the reverse charge movement is obvious. It is possible to offer an explanation of this reversal in the sign of $q(L_\sigma \rightarrow L_\pi)$ in terms of the intermolecular interactions, which differ quite strongly between the two types of compound.

In the Elpasolite crystal each nitrogen atom is surrounded by an axial potassium ion (C–N–K *ca.* 180°) and three close equatorial caesium ions (C–N–Cs *ca.* 90°). The overlap densities between the nitrogen atom and the potassium and the caesium ions at the experimental distances were calculated. The amounts are quite similar. Assuming the charge polarisation of the nitrogen atom is the result of overlap, we might expect that an equatorial/axial ratio of 2:1, as in octahedral complexes, would give no change from the carbon–nitrogen contribution, assumed constant. Then the *three* equatorial ions should give polarisation of the electron charge cloud in the direction of the *one* axial ion, *viz.* negative $q(L_\sigma \rightarrow L_\pi)$, as is observed.

On the other hand, in the cobalt ammine salts there is a *short* axial CN ··· H–N bond (210 pm) and three much longer (260 pm) such bonds approximately at right angles. This arrangement might well result in the axial N ··· H overlap dominating over the equatorial contributions, and hence a polarisation of the electron cloud in the opposite sense to that of the Elpasolite salt, *viz.* positive $q(L_\sigma \rightarrow L_\pi)$, as is observed.

Although very detailed calculations would be required to put the arguments of the previous paragraphs on a quantitative basis, we believe that the observed differences between the two types of compound in the nitrogen region are real and are to be explained in terms of intermolecular contacts. The spin-density results, also quoted in Table 5, agree fairly well with the DV-Xα calculations. We concluded[2,3] that covalence effects are not dominant in the spin-density distribution but that electron correlation influences it to a comparable extent. From the *X*-ray experiment, in addition to this, we may conclude that, while the broad picture of σ-bonding and π-backbonding effects is supported, 'intermolecular' contacts have a substantial influence on the charge density. These intermolecular effects appear to be quite short range in nature.

If we regard the crystal as merely an assemblage of atoms, then the chromium atom is modified by its nearest neighbours, six carbon atoms, the carbon atoms by the chromium and their associated nitrogen atom, and the nitrogen atoms by their nearest neighbours, the carbon partners having the strongest effect but the potassium and caesium neighbours are not unimportant. On this basis the agreement between theory and both experiments in the $Cr–C_6$ region is understandable, as is

Table 5. Results for some significant bonding parameters of the $[Cr(CN)_6]^{3-}$ ion. The population changes are related to an assembly of six unco-ordinated cyanide ions and a 'prepared' chromium $t_{2g}^3e_g^0$ atom. Overlap populations have been distributed between Cr d_σ and C_σ orbitals. The 'shell' populations also have been distributed

Population change (obs. assembly)	This experiment	Cobalt ammine–$Cr(CN)_6$ experiment [1]	*Ab initio* calculation [5] (RHF)	DV-Xα calculation [6] (charge)	Spin-density experiment [2,3]	DV-Xα calculation [6] (spin)
Cr d_π	−0.8(2)	−0.3(2)	−0.03	−0.12	−0.70(3)	−0.38
d_σ	1.0(6)	1.1(3)	0.81	1.28	0.12(4)	0.30
Diffuse	0.1(4)	0.5(5)	0.63	0.62	0.83(7)	0.12
Total charge	2.6(6)	1.8(5)	1.70	1.20	—	—
C σ	−0.1(3)	−0.1(2)	−0.19	−0.30	−0.04(1)	−0.07
π	−0.1(2)	−0.1(2)	0.09	0.07	−0.04(1)	−0.03
Total charge	−0.4(2)	−0.2(2)	−0.45	−0.17	—	—
N σ	0.1(3)	−0.2(2)	−0.03	−0.01	−0.03(1)	0.00
π	−0.3(2)	0.4(2)	−0.07	−0.03	0.09(1)	0.09
Total charge	−0.3(2)	−0.8(1)	−0.34	−0.53	—	—
Cr–C overlap	0.15(8)	0.15(5)	0.19	0.26	—	—
$q(L_\sigma \rightarrow M_\sigma)$	0.17(8)	0.18(5)	0.19(6)	0.22(1)	0.16(1)	0.07(1)
$q(M_\pi \rightarrow L_\pi)$	0.09(6)	0.06(4)	0.00(1)	0.02(1)	0.11(1)	0.06(1)
$q(L_\sigma \rightarrow L_\pi)$	−0.3(1)	0.2(1)	0.00(1)	0.01(1)	−0.08(2)	0.00(1)

the disagreement around the nitrogen atoms, which reflects the different environments in the crystals and is neglected in the theoretical calculations.

Acknowledgements

We are grateful to Dr. A. H. White and the Crystallographic Centre of this University for data collection, and to the Australian Research Grants Scheme for financial support.

References

1 B. N. Figgis and P. A. Reynolds, *Inorg. Chem.*, 1985, **24**, 1864.
2 B. N. Figgis, J. B. Forsyth, R. Mason, and P. A. Reynolds, *Chem. Phys. Lett.*, 1985, **115**, 454.
3 B. N. Figgis, J. B. Forsyth, and P. A. Reynolds, *Inorg. Chem.*, in the press.
4 L. G. Vanquickenborne, L. Haspelagh, M. Hendrickx, and J. Verhulst, *Inorg. Chem.*, 1984, **23**, 1677.
5 M. Sano, H. Kashiwagi, and H. Yamatera, *Inorg. Chem.*, 1982, **21**, 3827.
6 M. Sano, H. Adachi, and H. Yamatera, *Bull. Chem. Soc. Jpn.*, 1981, **54**, 2898.
7 B. N. Figgis, P. A. Reynolds, and A. H. White, *Inorg. Chem.*, 1985, **24**, 3762.
8 B. N. Figgis, P. A. Reynolds, and A. H. White, preceding paper.
9 B. N. Figgis, P. A. Reynolds, and S. Wright, *J. Am. Chem. Soc.*, 1983, **105**, 434.
10 J. M. Stewart and S. R. Hall (eds.), 'The XTAL System of Crystallographic Programs,' Computer Science Technical Report No. TR-901, University of Maryland, College Park, MD, 1983.
11 'International Tables for *X*-Ray Crystallography,' eds. J. A. Ibers and W. C. Hamilton, Kynoch Press, Birmingham, 1974, vol. 4.
12 D. T. Cromer and D. J. Liberman, *J. Chem. Phys.*, 1970, **53**, 1891.
13 B. N. Figgis, E. S. Kucharski, P. A. Reynolds, and A. H. White, *Acta Crystallogr., Sect. C*, 1983, **39**, 1587.
14 R. R. Ryan and B. I. Swanson, *Phys. Rev. B*, 1976, **13**, 5320.
15 S. R. Fletcher and T. C. Gibb, *J. Chem. Soc., Dalton Trans.*, 1977, 309.
16 P. J. Brown, M. Favas, B. N. Figgis, and J. B. Forsyth, *Aust. J. Chem.*, in the press.
17 B. N. Figgis, P. A. Reynolds, and G. A. Williams, *Acta Crystallogr., Sect. B*, 1981, **37**, 504.
18 P. E. Cade, W. F. Huo, and J. B. Greenshields, *At. Data Nucl. Data Tables*, 1975, **15**, 1.
19 E. Clementi and C. Roetti, *At. Data Nucl. Data Tables*, 1974, **14**, 187—267.
20 J. W. Bats and D. Feil, *Chem. Phys.*, 1977, **26**, 79.
21 M. E. Stephens and P. J. Becker, *Mol. Phys.*, 1983, **49**, 65.
22 B. N. Figgis and P. A. Reynolds, *Int. Rev. Phys. Chem.*, 1986, **5**, 265.

Received 30*th June* 1986; *Paper* 6/1304